

1998

Femtosecond Photoemission Study of Ultrafast Electron Dynamics in Single-Crystal Au(111) Films

J. Cao

Y. Gao


H. E. Elsayed-Ali

Old Dominion University, helsayed@odu.edu

R. J. D. Miller

D. A. Mantell

Follow this and additional works at: http://digitalcommons.odu.edu/ece_fac_pubs

 Part of the [Condensed Matter Physics Commons](#), and the [Electrical and Computer Engineering Commons](#)

Repository Citation

Cao, J.; Gao, Y.; Elsayed-Ali, H. E.; Miller, R. J. D.; and Mantell, D. A., "Femtosecond Photoemission Study of Ultrafast Electron Dynamics in Single-Crystal Au(111) Films" (1998). *Electrical & Computer Engineering Faculty Publications*. 120.
http://digitalcommons.odu.edu/ece_fac_pubs/120

Original Publication Citation

Cao, J., Gao, Y., Elsayed-Ali, H. E., Miller, R. J. D., & Mantell, D. A. (1998). Femtosecond photoemission study of ultrafast electron dynamics in single-crystal Au(111) films. *Physical Review B*, 58(16), 10948-10952. doi:10.1103/PhysRevB.58.10948

Femtosecond photoemission study of ultrafast electron dynamics in single-crystal Au(111) films

J. Cao* and Y. Gao

Center for Photoinduced Charge Transfer and Department of Physics and Astronomy, University of Rochester, Rochester, New York 14627

H. E. Elsayed-Ali

Department of Electrical and Computer Engineering, Old Dominion University, Norfolk, Virginia 23529

R. J. D. Miller

Departments of Chemistry and Physics, 60 St. George Street, University of Toronto, Toronto, Ontario, Canada M5S 1A7

D. A. Mantell

Webster Research Center, Xerox Corporation, Webster, New York 14580

(Received 17 February 1998)

The energy-dependent relaxation of photoexcited electrons has been measured by time-resolved two-photon photoemission spectroscopy on single-crystal Au(111) films with thickness ranging from 150 to 3000 Å. It is found that the energy-dependent relaxation does not show any significant thickness dependence, which indicates that electron transport is a much slower dynamical process in the near-surface region than expected from bulk properties. Furthermore, lifetimes of the photoexcited electrons can be fitted well by the Fermi-liquid theory with a scaling factor plus an effective upper lifetime. This observation enables separation of electron-electron scattering, and to a lesser extent electron-phonon scattering, processes from electron-transport effects on the surface dynamics. [S0163-1829(98)04840-1]

Recently, the ultrafast dynamics of excited electrons on metal surfaces has become an active area of investigation due to the development of femtosecond time-resolved surface-sensitive techniques. Time-resolved two-photon photoemission (TR-TPPE) has been used as an approach to measure the energy-dependent lifetimes of the photoexcited electrons on different metal surfaces.¹⁻⁶ It is found that the relaxation lifetimes of photoexcited electrons are in the femtosecond time scale and decrease rapidly with their excitation energy above the Fermi level (E_F), depending upon the specific band structure. For the higher excited states (with excitation energy larger than 0.5 eV above the E_F), the ultrashort electron lifetimes can be attributed to the strong electron-electron scattering processes due to the large available phase space. However, for the low-excitation states very close to the Fermi level, the relaxation mechanism is still unclear. This is because several other relaxation mechanisms besides electron-electron scattering have to be considered. First, since the lifetimes of these low-energy electrons become infinitely long as they approach E_F according to the Fermi-liquid theory (FLT) for electron-electron scattering,^{7,8} other scattering mechanisms, such as electron-phonon scattering (e - p) and scattering by defects, become more important or even dominant. Second, when excited electrons are generated by absorption of an optical pulse, the exponential population gradient that results from linear absorption leads to diffusive and ballistic motion of the excited electrons away from the optically probed surface region. This electron transport provides an additional decay component to the photoexcited electron population at the surface, and could impose an upper lifetime limit to the study of electron dynamics by surface-sensitive time-resolved two-photon

photoemission. Therefore, to understand the relaxation processes at these lower excited states, an experiment capable of identifying the role of each of these mechanisms is required.

In this paper, we present femtosecond time-resolved photoemission studies of electron dynamics on single-crystal Au(111) films, epitaxially grown on mica, with thicknesses ranging from 150 to 3000 Å. For the 150-Å film, since its thickness is comparable to the optical probe depth (170 Å for 3.2-eV photons in gold) and the mean free path of photoelectrons (120 Å for photoelectrons with energies 3.2 eV above E_F), the photoexcited electrons are spatially confined within the surface-probed region and the relaxation from electron transport is greatly reduced or even completely eliminated. Therefore, the lifetimes of the photoexcited electrons are solely determined by the scattering processes (electron-electron and, to a lesser extent, electron-phonon) other than transport. In addition, by measuring the dependence of electron relaxation on the film thickness, the contribution of electron transport to the population decay of the lower-energy electrons, excited slightly above the Fermi level, can be investigated. This approach enables the transport contribution to be separated from the electron relaxation through scattering. We find that the electron transport is a much slower dynamical process in the near-surface region than expected from bulk properties, and lifetimes of the photoexcited electrons can be fitted well by the Fermi-liquid theory with a scaling factor plus an effective upper time limit.

The TR-TPPE technique used to measure surface electron dynamics is described in more detail elsewhere.^{2,6,10} Briefly, the output pulse of a Ti:sapphire laser (photon energy 1.45–1.70 eV, pulse width 40 fs, and repetition rate 82 MHz) is first frequency doubled with a 250- μ m-thick beta barium

borate doubling crystal. The doubled light (photon energy 2.9–3.4 eV) is then split by an equal-intensity beam splitter. One beam serves as a pump pulse to generate excited electrons in the sample, while the other, passing through a variable delay line, is used as a probe pulse to photoemit the excited electrons. The relative polarizations of the pump and probe beams can be changed by a zero-order half-wave plate inserted in one beam path. By recording the photoelectron intensity from each specific excited electronic state of the sample as a function of the pump-probe delay time, the relaxation of the excited electrons can be directly observed. The laser pulse energy was kept very low, at about 0.5 nJ/pulse, and on average less than one electron per pulse was photoemitted. The electronic temperature rise due to the laser pulse irradiation was estimated less than 10 K (0.5 nJ/pulse and 150 μm beam diameter). This low-pulse-energy and high-repetition-rate measurement provides high sensitivity and more reliable detection by eliminating the ambiguities that might arise in a highly excited electron distribution, from effects such as thermionic emission, or space-charge factors.

Au(111) single-crystal films were fabricated by epitaxial growth on mica substrates by thermal evaporation in a separate ultrahigh-vacuum chamber. The film thickness was determined by a crystal thickness monitor with an estimated absolute accuracy better than $\pm 20\%$ of the film thickness. In order to obtain an atomically clean surface, each sample was degassed in the UHV testing chamber with a base pressure of 5×10^{-11} torr at 750 K for several hours, and flashed to 1000 K for a few seconds to remove the surface contaminants introduced during transport in the open air. After this treatment, carbon contaminant was not detectable, and the estimated oxygen coverage was less than 0.05 ML based on x-ray photoelectron spectroscopy (XPS) peak-intensity calculations. Reflection high-energy electron diffraction showed sharp single-crystal patterns with (111) orientation.

A two-photon photoemission spectrum from an Au(111) surface after the flash-heating treatment is shown in Fig. 1. The spectrum was taken with photon energy of 3.2 eV at an energy resolution of 0.1 eV. The surface work function Φ is determined from $\Phi = 2h\nu - W$, where W is the measured spectral width. The typical work function of flashed Au(111) was 5.1 eV, which is within 0.3 eV of that published by another group.⁹

The clean Au(111) surface was first dosed with Cs to lower the surface work function. This enables lifetime measurements of the lower excited states, within 0.3 eV above E_F , with photon energies smaller than the intrinsic surface work function. The final alkali metal coverage is estimated to be less than 0.1 ML based on the work-function measurement and the XPS peak-intensity calculation. The perturbation to the electron dynamics after the alkali metal deposition has been investigated on the lifetime measurements on the Cu(100) surface⁶ covered with different alkali metals (K and Cs), where no discrepancy of lifetime measurement within one-photon energy above the Fermi level was observed. In addition, the lifetime measurements do not show any observable difference compared with the clean Au(111) surface within the overlapping energy range $2.0 < (E_i - E_F) < 3.2$ eV. A two-photon photoemission spectrum of Cs-covered Au(111) surface taken with photon energies of 3.2 eV is also

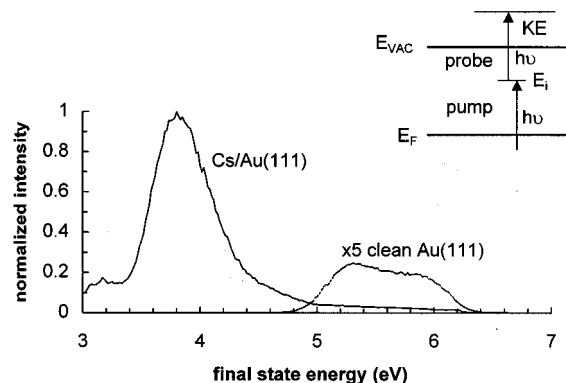


FIG. 1. Two-photon photoemission spectra of Au(111) taken with a photon energy of 3.2 eV. Solid and dotted lines represent spectra from Cs-covered and clean Au(111) surfaces, respectively. The schematic of the two-photon photoemission process is shown in the inset.

shown in Fig. 1. The shape of the spectrum reflects the electronic band structure of the Au(111) surface. The flat part at the high-energy side is the two-photon photoemission from Au 6s electrons (*s-p* band), and the peak at the lower energy is from Au 5d electrons with its rising edge at about 2.0 eV below E_F .⁷

The lifetime measurements were carried out right after alkali metal deposition by taking pump-probe scans at various kinetic energies of the two-photon photoemission spectrum. The polarizations of the pump and probe beams were kept perpendicular to each other (*s* and *p* polarized) in order to minimize the coherence peak.^{6,10} The corresponding energies of the intermediate states (E_i) are determined by assigning the Fermi edge in the two-photon photoemission spectrum (E_{KMAX}) as the highest excited intermediate state, with one-photon energy above E_F , i.e., $E_i = E_K - E_{KMAX} + E_F + h\nu$, where E_K is the measured kinetic energies of photoelectrons. The extraction of the lifetimes from each pump-probe scan follows our previous protocol used in the lifetime measurements on copper surfaces.⁶ Briefly, for the highest excited electrons, their lifetimes are very short and the corresponding pump-probe scans are fitted by the convolution of a single exponential decay function with the instrument response function. For lower excitation states slightly above the Fermi level, a simple exponential decay no longer holds since the electron relaxation from the higher levels into the lower lying levels contributes to the population dynamics. This repopulation process was modeled by a simplified three-level system, which is described in more detail elsewhere for similar relaxation processes.^{6,10} This method enables the separation of the repopulation contribution to the electron relaxation processes from the intrinsic relaxation due to *e-e* scattering at the lower excited states very close to the Fermi level, and the extraction of the intrinsic electron lifetimes. A pump-probe scan taken from the excited state with energy of 0.3 eV above the Fermi level of the Cs-covered 150 Å Au(111) film is shown in the inset of Fig. 2. Since the two-photon photoemission yield for *s*-polarized light is about six times smaller than that of the *p*-polarized light in our experiments, the nonlinear repopulation process causes the two-photon photoemission signal to be weaker

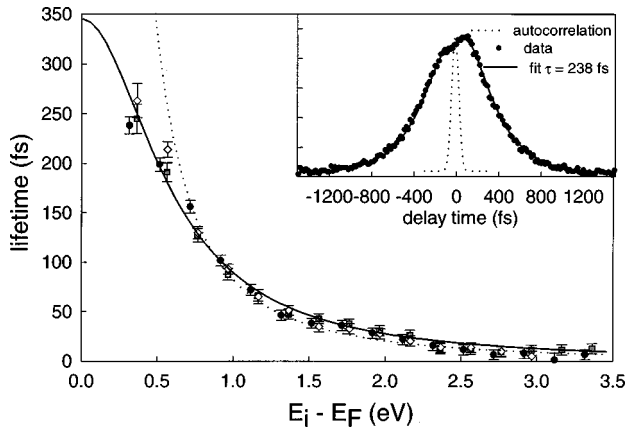


FIG. 2. Lifetime measurements of single-crystal Au(111) films with different thicknesses. The error bars are one standard deviation. Filled circles, shaded squares, and open diamonds represent lifetime measurements from films with thicknesses of 150, 500, and 3000 Å, respectively. The solid line is the best fit from Eq. (1) with $z = 6.5 \pm 0.6$ and $\tau_1 = 345 \pm 32$ fs. The dotted line is the best fit with Fermi liquid theory alone ($z = 4.0 \pm 0.4$) for the energy range 0.7–3.2 eV above the E_F . A pump-probe scan taken from the excited state with energy of 0.3 eV above the Fermi level of Cs-covered 150-Å Au(111) film is shown in the inset. Its lifetime was fitted to be $\tau = 238 \pm 10$ fs.

when the s beam is the pump and the p beam is the probe than p pump and s probe. This asymmetry in the pump-probe signal near zero time delay becomes stronger as the probed intermediate levels get closer to the Fermi level, where the repopulation process makes a larger contribution to the dynamics. This asymmetry serves as a fingerprint for the repopulation process in the cross-polarized TR-TPPE experiment.

The relaxation of photoexcited electrons as a function of their energies for Au(111) films with thicknesses of 150, 500, and 3000 Å are summarized in Fig. 2. Several results are noteworthy. First, for most of the excited-state energy range (0.7–3.2 eV above E_F), the lifetime energy dependence exhibits very good Fermi-liquid behavior, i.e., $\tau \propto (E_i - E_F)^{-2}$. Second, the anomalous feature associated with the photoexcitation of d electrons also exists at about the same energy position (about 1.7 eV above the Fermi level) as in copper.⁶ This effect is observable as a small change in slope, which is discernible in Fig. 2 as a longer-lived deviation from the best fit to the FLT predictions (dotted line). However, this feature is much weaker than that in copper, and we believe this difference is because the Au 5d electrons lie further away from the nucleus than Cu 3d electrons and are less localized. Third, the energy-dependent relaxation of photoexcited electrons does not show any noticeable thickness dependence. Single-crystal films were used explicitly to minimize the chances of electron scattering from grain boundaries and defects, and to explore the effects of hot-electron transport on the surface dynamics. The lack of any significant thickness dependence, over a range larger than 20 times that of the surface probe depth (~ 120 Å), indicates that the hot-electron transport away from a metal surface is a much slower process in comparison with the scattering relaxation mechanisms.

Under the low-excitation condition, the excited electrons

in metals relax mainly through scattering with cold conduction-band electrons. Theoretical predictions for this energy-dependent relaxation process are generally calculated using Landau's Fermi-liquid theory.⁷ The FLT prediction of electron lifetime due to electron-electron scattering based on the work of Quinn⁸ by using a jellium model is given by $\tau_{FLT} = 18.38(E_i - E_F)^{-2}$ (in fs), where the energy is in eV. Lumping all the other contributions (e - p scattering and electron transport) to the population decay into an effective decay constant τ_1 , the lifetimes of photoexcited electrons measured in the TR-TPPE can be modeled as

$$\frac{1}{\tau} = \frac{1}{\tau_1} + \frac{1}{z\tau_{FLT}}. \quad (1)$$

The best fit of Eq. (1) to the experimental results for all the films is shown as a solid line in Fig. 2, with $z = 6.5 \pm 0.6$ and $\tau_1 = 345 \pm 32$ fs. We believe that the scaling factor 6.5 arises mainly from the fact that only the 6s electrons are included in the calculation and the screening of the 5d electrons is neglected. These observations should be compared to the similar results obtained from earlier time-resolved photoemission studies of the electron thermalization in a 300-Å polycrystalline Au film by Fann *et al.*¹ They found that the evolution of the electron-energy distribution from the nascent nonthermal distribution generated by an intense pump pulse to a hot Fermi-Dirac distribution can qualitatively be described by FLT within a factor of 5.

For single-crystal metal films, the mechanisms that make the most significant contributions in determining the effective lifetime τ_1 are electron-photon scattering and electron transport. In gold at room temperature, the average e - p scattering time is about 30 fs, and on average an electron loses about 15 meV (Debye temperature is 170 K) to create a phonon after each collision.⁷ Therefore, it will take about ten consecutive scattering events for an excited electron to lose more than 0.1 eV to escape out of the probe window of the energy analyzer (0.1 eV). The corresponding upper lifetime limit through this electron-phonon scattering is about 300 fs, which is the same order of τ_1 .

The hot-electron transport in gold has also been studied by several groups^{11–14} using transient thermorefectivity and thermotransmissivity. In these measurements, the front surface of a thin metal film was excited by an intense ultrashort laser pulse (intensity usually larger than 10^{10} W/cm²), and the change in optical reflectivity or transmissivity at both front and back surfaces was recorded as a function of delay time between the pump and probe pulses. The delay time of the rising edge in the reflectivity modulation for the back-surface probe was found to increase with the sample thickness in a manner that is consistent with ballistic electron transport away from the surface region with a velocity of about 10^8 cm s⁻¹, i.e., the same order of magnitude as the Fermi velocity of electrons in gold, 1.4×10^8 cm s⁻¹.

These studies prompted us to examine the effect of ballistic transport on the measured electron dynamics with TR-TPPE. A theoretical calculation, based on a one-dimensional ballistic-transport model was performed for the semi-infinite sample.¹⁵ The basic assumptions of this model are that the photoexcited electrons are free to move isotropically in all directions at the Fermi velocity without suffering any colli-

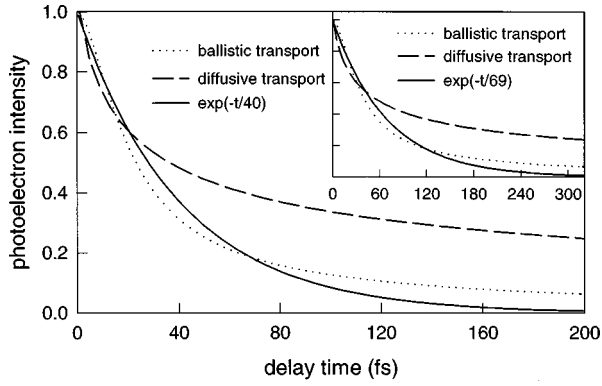


FIG. 3. Calculation of the effect of electron transport on the lifetime measurements of photoexcited electrons on the surface region with TR-TPPE. The dotted line is the photoelectron intensity as a function of delay time between pump and probe pulses after ballistic transport. In this calculation the optical skin depth was 170 Å for 3.2-eV photons and the escape depth of the photoelectrons was 110 Å for the electrons with 3.4-eV final energy (or 0.2-eV intermediate) above E_F . The solid line is a fit using a single exponential decay and gives an effective decay time of about 40 fs. The calculation of the effect of ballistic transport in front reflectivity measurements is shown in the inset. Assuming strictly diffusive surface transport, the decay times are expected to be ~ 85 and ~ 120 fs for surface TR-TPPE and front-surface reflectivity studies, respectively.

sions, and at the surface they undergo total elastic reflections. The isotropic transport assumption is based upon the fact that the band structure of Au in the vicinity of the Fermi level is very much free-electron-like⁷ and the electronic temperature rise (less than 10 K) due to laser irradiation is small and will not significantly perturb this band structure. Since the laser-excited area (beam diameter 150 μm) is much larger than both the optical skin depth (170 Å for 3.2 eV photons) and the mean free path of photoelectrons (110 Å for electrons at 3.4 eV above E_F), the electron transport along the surface direction can be neglected on the ultrafast time scale (fs to ps). The contribution of electron transport away from the surface is calculated by the projection of the three-dimensional distribution function to the surface normal direction (one dimension). The effect of the finite mean free path of the photoelectrons is also included in the calculation. The calculation of photoelectron intensity as a function of the pump and probe delay time after this ballistic electron transport is shown in Fig. 3, which gives an upper lifetime limit to the excited electron population decay in the surface region of approximately 40 fs. This effective lifetime is much shorter than the lifetime of 290 fs for an electron at 0.2 eV above the Fermi level, obtained by extrapolating the experimental lifetime-energy dependence curve. The same calculation was also performed for the case of front surface reflectivity experiments with an optical skin depth of 150 Å and an electron velocity of $1.4 \times 10^8 \text{ cm s}^{-1}$ (Fermi velocity in gold), and the results are shown in the inset of Fig. 3 with the effective decay time of ~ 69 fs.

In comparing the predicted decay in the surface distribution of photoexcited electrons to the experimental results, as a function of crystal thickness, it is clear that transport is not contributing significantly to the dynamics. The absence of

this component to the electron dynamics is intriguing as it is clearly observed in the transient (back surface) reflectivity studies. The resolution of this discrepancy between the photoemission and the transient reflectivity might be found in the difference of experimental methods being used. When optical probes are used to study surface electron dynamics, the observables are the macroscopic optical constants and theoretical models are needed to extract electron dynamical information from the observed changes in optical properties. Therefore, these techniques generally do not provide a direct measurement of the electron dynamics, as time-resolved two-photon photoemission does. Due to the relatively low sensitivity of optical probes, more intense laser pulses are used in thermorefectivity experiments, which induces significant lattice heating. As a result, electron-phonon coupling must be considered in order to extract information about the electron dynamics. Under the very high excitation density (higher than 10^{10} W/cm^2) and nonthermal conditions, it might be statistically possible that some of the hot electrons transport more or less ballistically while the majority do not. For example, considering the average e - p collision time of 30 fs, it is possible for some of the lower excited electrons slightly above E_F with Fermi velocity ($\sim 14 \text{ Å/fs}$) to transverse across a film (thickness of 3000 Å) without suffering any significant collisions. Thus, the optical measurements of the rising edge of the thermal modulation signal might mainly recover the ballistic portion of the electron transport. In the present measurements, almost no lattice heating was involved due to the much lower laser pulse intensity used (less than 10^8 W/cm^2). Furthermore, with highly surface-sensitive time-resolved two-photon photoemission, we measure the residue of hot electrons after transport, and this ballistic transport portion will be a much smaller component to the total population decay.

It is worth noting that even the decays from the front surface reflectivity do not show a decay component that would correspond to the ballistic transport, which is estimated at about 69 fs (see inset of Fig. 3), to the electron population decay at the surface region.¹² The measured reflectivity decay time constants are about 1 and 2 ps for 200- and 2000-Å films for their front-surface pump-probe data, which gives ~ 2 ps effective decay time for the transport contribution. This is comparable to our results observed in the TR-TPPE experiments. This decay in the near-surface distribution is even slower than that expected for completely diffusive motion of the electron distribution. Assuming bulk parameters⁷ (diffusivity $D = K/C_e$, where K (310 W/m K) is the electron thermal conductivity, and C_e (18.4 J/m³ K) is the electron specific heat at room temperature), the diffusive transport should lead to a $1/e$ decay time of approximately 85 and 120 fs for TR-TPPE and time-resolved front-surface reflectivity, respectively. Again, the upper lifetime limit and lack of crystal thickness dependence do not show a transport component of this magnitude. Several processes might contribute, in part, for this observed slower transport phenomenon. First, the initial excitation in gold with 3.2-eV photons involves predominately direct transition from the d -band to the sp band. Subsequent relaxation of the d holes will generate excited electrons through the Auger process that lies in the energy range probed in the experiment. The measured relaxation processes will thus be influenced by the relaxation

of the hot holes also. Since these holes are strongly localized, they will be affected to a much lesser extent by transport, compared to *sp* electrons (or *sp* holes), due to the small dispersion in the *d* band. However, the high-resolution angle-resolved photoemission study of *d*-hole lifetimes in copper¹⁶ reveals that their lifetimes are in the order of ~ 50 fs, the same lack of thickness dependence on the lifetime measurements of copper thin films with thicknesses ranging from 200 to 3000 Å (Ref. 15) implies that the *d*-hole contributions to the slow transport would not be significant. Second, the re-population of lower excited states by the secondary electrons

generated through the relaxation of higher excited states will, in some extent, compensate for the decay of the electron population in the near-surface region due to transport loss. Further studies are needed to completely understand this interesting observation.

The authors would like to thank C. A. Schmuttenmaer for helpful discussions. This work was funded by National Science Foundation Grant No. CHE-9120001. R.J.D.M. would like to acknowledge support from the Natural Sciences and Engineering Research Counsel of Canada (Grant No. OGP0183702).

*Present address: Chemistry Department, California Institute of Technology, Mail Code 127-72, Pasadena, CA 91125.

¹W. S. Fann, R. Storz, H. W. K. Tom, and J. Bokor, Phys. Rev. Lett. **68**, 2834 (1992); Phys. Rev. B **46**, 13 592 (1992).

²C. A. Schmuttenmaer, M. Aeschlimann, H. E. Elsayed-Ali, R. J. D. Miller, D. A. Mantell, J. Cao, and Y. Gao, Phys. Rev. B **50**, 8957 (1994).

³T. Hertel, E. Knoesel, M. Wolf, and G. Ertl, Phys. Rev. Lett. **76**, 535 (1996); E. Knoesel, A. Hotzel, T. Hertel, M. Wolf, and G. Ertl, Surf. Sci. **386**, 76 (1996).

⁴M. Aeschlimann, M. Bauer, and S. Pawlik, Chem. Phys. **205**, 127 (1996).

⁵S. Ogawa, H. Nagano, and H. Petek, Phys. Rev. B **55**, 10 869 (1997).

⁶J. Cao, Y. Gao, R. J. D. Miller, H. E. Elsayed-Ali, and D. A. Mantell, Phys. Rev. B **56**, 1099 (1997).

⁷N. W. Ashcroft and N. D. Mermin, *Solid State Physics* (Holt,

Rinehart and Winston, New York, 1976).

⁸J. J. Quinn, Phys. Rev. **126**, 1453 (1962).

⁹H. B. Michaelson, J. Appl. Phys. **48**, 4729 (1977).

¹⁰C. A. Schmuttenmaer, C. C. Miller, J. Herman, J. Cao, D. A. Mantell, Y. Gao, and R. J. D. Miller, Chem. Phys. **205**, 91 (1996).

¹¹R. W. Schoenlein, W. Z. Lin, J. G. Fujimoto, E. P. Ippen, and G. L. Eesley, Phys. Rev. Lett. **58**, 1680 (1987).

¹²S. D. Brorson, J. G. Fujimoto, and E. P. Ippen, Phys. Rev. Lett. **59**, 1962 (1987).

¹³T. Juhasz, H. E. Elsayed-Ali, G. O. Smith, C. Suárez, and W. E. Bron, Phys. Rev. B **48**, 15 488 (1993).

¹⁴C. Suárez, W. E. Bron, and T. Juhasz, Phys. Rev. Lett. **75**, 4536 (1995).

¹⁵J. Cao, Ph.D. thesis, University of Rochester, 1996.

¹⁶R. Matzdorf, R. Paniago, G. Meister, and A. Goldman, Solid State Commun. **92**, 839 (1994).